



Short communication

Technical note: Aerosol light absorption measurements with a carbon analyser – Calibration and precision estimates



B.A.J. Ammerlaan^{a, b}, R. Holzinger^b, A.D. Jedynska^a, J.S. Henzing^{a, *}

^a Netherlands Institute for Applied Scientific Research (TNO), Utrecht, The Netherlands

^b Institute for Marine and Atmospheric Research Utrecht (IMAU), Utrecht University, Utrecht, The Netherlands

HIGHLIGHTS

- On the application of a carbon analyser as absorption photometer.
- Measuring the mass absorption efficiency with a single instrument.
- Determination of the precision of mass absorption efficiency.

ARTICLE INFO

Article history:

Received 16 September 2016

Received in revised form

10 May 2017

Accepted 16 May 2017

Available online 25 May 2017

Keywords:

Black carbon

Elemental carbon

Aerosol light absorption

Mass absorption efficiency

ABSTRACT

Equivalent Black Carbon (EBC) and Elemental Carbon (EC) are different mass metrics to quantify the amount of combustion aerosol. Both metrics have their own measurement technique. In state-of-the-art carbon analysers, optical measurements are used to correct for organic carbon that is not evolving because of pyrolysis. These optical measurements are sometimes used to apply the technique of absorption photometers. Here, we use the transmission measurements of our carbon analyser for simultaneous determination of the elemental carbon concentration and the absorption coefficient. We use MAAP data from the CESAR observatory, the Netherlands, to correct for aerosol-filter interactions by linking the attenuation coefficient from the carbon analyser to the absorption coefficient measured by the MAAP. Application of the calibration to an independent data set of MAAP and OC/EC observations for the same location shows that the calibration is applicable to other observation periods. Because of simultaneous measurements of light absorption properties of the aerosol and elemental carbon, variation in the mass absorption efficiency (MAE) can be studied. We further show that the absorption coefficients and MAE in this set-up are determined within a precision of 10% and 12%, respectively. The precisions could be improved to 4% and 8% when the light transmission signal in the carbon analyser is very stable.

© 2017 The Authors. Published by Elsevier Ltd. This is an open access article under the CC BY-NC-ND license (<http://creativecommons.org/licenses/by-nc-nd/4.0/>).

1. Introduction

Black carbon is a qualitative description when referring to light absorbing carbonaceous substances in atmospheric aerosol. Black carbon can be related to some measurable properties that together with the suitable method define the terminology (Bond et al., 2013; Petzold et al., 2013). The most commonly measured properties are elemental carbon (EC), a mass metric, and the absorption coefficient, determined by light absorption. The absorption coefficient is commonly converted into a mass metric by application of a mass-specific absorption cross section (MAC; referred to as mass

absorption efficiency, MAE hereafter). The mass metric based on light absorption measurement is to be referred to as equivalent black carbon (EBC).

Elemental carbon (EC) and organic carbon (OC) are quantified by thermal-optical analysis. In the analyser, e.g. the Sunset Laboratory Inc. Thermal Optical Carbon Aerosol Analyser (Sunset Laboratory Inc, Tigard, USA) and the DRI Thermal Optical Carbon Analyser (Atmoslytic, Inc., Calabasas, USA), a filter punch is heated in an oven by a thermal programme, e.g. EUSAAR2 (Cavalli et al., 2010), NIOSH890 (Peterson and Richards, 2002) or IMPROVE_A (Chow et al., 2007). The separation between OC and EC is based on the thermal and chemical stability of the aerosol. During heating some particulate OC and absorbed organic vapours are converted to EC through pyrolysis in a pure helium atmosphere. Reflected or transmitted laser light is used to monitor and correct for this so

* Corresponding author.

E-mail address: bas.henzing@tno.nl (J.S. Henzing).

called pyrolytic carbon (PC) (Turpin et al., 1990).

In monitoring networks, the absorption coefficient is generally measured with absorption photometers, e.g. the Aethalometer (AE; Magee Scientific, Berkeley, USA; Hansen et al., 1984), the Particle Soot Absorption Photometer (PSAP; Radiance Research, Seattle, USA) and the Multi-Angle Absorption Photometer (MAAP; Thermo Fisher Scientific, Waltham, USA; Petzold and Schönlinner, 2004). Absorption photometers continuously measure the attenuation of light by the aerosol and filter. To finally obtain the absorption coefficient of the aerosol in ambient air, corrections need to be performed to the attenuation coefficient, to account for aerosol-filter interactions. Different correction algorithms are used for Aethalometer (e.g. Weingartner et al., 2003; Arnott et al., 2005; Collaud Coen et al., 2010) and PSAP (Bond et al., 1999; Virkkula et al., 2005; Müller et al., 2014). The MAAP measures, besides the transmission, also the reflection at two different angles. The measured reflection and transmission signals are used in a radiative transfer model to calculate the absorption caused by particles (Petzold and Schönlinner, 2004).

Ram and Sarin (2009) introduced the first method exploiting the transmission measurements of a thermal-optical analyser to infer the light absorption coefficient. They used a correction used by Weingartner et al. (2003) and Bond et al. (1999) to correct for a multiple scattering enhancement and a loading effect in the Aethalometer. The multiple scattering enhancement and the loading effect are parametrised by the factors C and $R(\text{ATN})$, respectively. The absorption coefficient is calculated by

$$b_{\text{abs}} = \frac{b_{\text{ATN}}}{C \cdot R(\text{ATN})} \quad (1)$$

Ram and Sarin (2009) used $C = 2.14 \pm 0.21$ and the function for $R(\text{ATN})$ as found by Weingartner et al. (2003), although they acknowledged that the value for C may not be optimal, because this value is determined for fresh diesel aerosol. Later, Andersson et al. (2011) used $C = 3.6 \pm 0.6$, which is determined for internally mixed aerosol. Collaud Coen et al. (2010) showed that the value of C is site specific. Therefore, we chose not to use one of these values for C . We chose to use a MAAP as reference instrument, because these instruments are widely available at monitoring stations. Furthermore, the MAAP has a low unit-to-unit variability of 3% (Müller et al., 2011), which is sufficient for the method and means that the calibrations can be performed by different instruments with a high reproducibility. An in-depth review of light absorption measurement methods is provided by Moosmüller et al. (2009).

The advantage of using the carbon analyser as absorption photometer is that both elemental carbon concentration and absorption coefficient can be determined by a single instrument. This enables the calculation of the mass absorption efficiency of EC (MAE, in $\text{m}^2 \text{g}^{-1}$) that is crucial for aerosol climate impact studies. The mass absorption efficiency is calculated by

$$\text{MAE} = \frac{b_{\text{abs}}}{\text{EC}} \quad (2)$$

Section 2 describes the used method and the calibration we added to the method of Ram and Sarin (2009). In Sect. 3, we calibrate the attenuation coefficient data inferred from the carbon analyser from a field campaign at the CESAR observatory near Cabauw, the Netherlands, performed in September and October 2014 and used an independent data set from June and July 2010 from the same site to validate the calibration. Finally, the results are discussed in Sect. 4.

2. Method

2.1. Attenuation coefficient

The optical attenuation of light (ATN) is defined as

$$\text{ATN} \equiv \ln\left(\frac{I_0}{I}\right) \quad (3)$$

where I_0 is the intensity of the incident laser beam and I is the intensity of the light passing through the filter.

With a carbon analyser, the attenuation cannot be determined directly, because the initial laser intensity I_0 is unknown. However, the difference in attenuation ΔATN , which is linked to the absorption, can be measured and is given as

$$\Delta \text{ATN} = \ln\left(\frac{I_0}{I_{T_d}}\right) - \ln\left(\frac{\eta I_0}{I_{T_w}}\right) = \ln\left(\frac{I_{T_w}}{I_{T_d}}\right) - \ln\left(\frac{\eta I_0}{I_0}\right) \approx \ln\left(\frac{I_{T_w}}{I_{T_d}}\right) \quad (4)$$

where I_{T_w} is the intensity of the transmitted light passing through a white filter, I_{T_d} is the intensity of the transmitted light through a laden, and thus dark, filter and η the variation of the incident beam in time. η is assumed to be close to 1 during the analysis, so the second logarithm, $\ln(\eta I_0/I_0)$, is negligible. Because the carbon analyser measures the intensity of the transmitted light through the white and laden filter, the difference in attenuation is a measurable quantity.

The first step in obtaining ΔATN is performing an OC/EC analysis with a carbon analyser according to an analysis protocol. After the measurement, the OC and EC mass concentrations can be calculated with the calculating software of the manufacturer of the instrument.

We obtained I_{T_d} by averaging the transmission signal over the first 60 s of the analysis, in this 60 s the filter is still dark and pyrolysis has not occurred yet. I_{T_w} is obtained by a measurement of the transmission signal for a white filter. This can either be at the end of the analysis protocol when all carbon has evolved from the filter or a blank filter from the same batch.

The measured difference in attenuation is expressed in the attenuation coefficient $b_{\text{ATN,Sunset}}$ (with the units of m^{-1}):

$$b_{\text{ATN,Sunset}} = \frac{A}{Q} \frac{\Delta \text{ATN}}{\Delta t} = \frac{A}{V} \ln\left(\frac{I_{T_w}}{I_{T_d}}\right) \quad (5)$$

Where A is the filter area (in m^2), Q is the volumetric flow rate (in $\text{m}^3 \text{s}^{-1}$) and Δt is the sampling time (in s). In the last step, the total sampled volume $V \equiv Q \Delta t$ (in m^3) is included. The factor A/V now represents the inverted column of air that is put onto the filter.

2.2. Calibration to absorption photometer

The measured attenuation differs from the absorption of the aerosols in air. This is caused by a multiple scattering enhancement (Liou et al., 1993; Ballach et al., 2001) and a loading effect, which is sometimes also referred to as ‘shadowing effect’ (Reid et al., 1998). To correct for these artefacts, a correction function $C \cdot R(\Delta \text{ATN})$ is introduced by e.g. Weingartner et al. (2003), where C parametrises the multiple scattering enhancement and $R(\Delta \text{ATN})$ parametrises the loading effect. There are more recent and more complex corrections available (Collaud Coen et al., 2010; Müller et al., 2014). However, the correction function proposed by Weingartner is simple and the more recent corrections perform only slightly better, but add more complexity.

In the calibration, the attenuation coefficient from the carbon

analyser is calculated according to Eq. (5). The recorded equivalent black carbon mass concentration from the MAAP is averaged over the same sampling time (Δt) as the filters for OC/EC analysis. To obtain the absorption coefficient from the MAAP, we have to undo the conversion to EBC by multiplying the reported EBC mass with the internal conversion factor of $6.6 \text{ m}^2 \text{ g}^{-1}$. The so obtained averaged absorption coefficient is called $b_{\text{abs,MAAP}}$. The attenuation coefficient $b_{\text{ATN,Sunset}}$ for a specific measurement is linked to co-located $b_{\text{abs,MAAP}}$ from the same sampling period. Figs. 1 and 2 demonstrate this method and show how a fit through these linked coefficients determines the correction factor or calibration factor $C \cdot R(\Delta \text{ATN})$.

2.3. Absorption coefficient and mass absorption efficiency

After a calibration to the MAAP, the absorption coefficient of aerosols measured with the carbon analyser can be calculated for future and past data as

$$b_{\text{abs,Sunset}} = \frac{b_{\text{ATN,Sunset}}}{C \cdot R(\Delta \text{ATN})} \quad (6)$$

where b_{ATN} is the attenuation coefficient as determined in Eq. (5) and $C \cdot R(\Delta \text{ATN})$ is the correction factor as determined in Sect. 2.2.

Using $b_{\text{abs,Sunset}}$ and the elemental carbon concentration from these instruments (EC in $\mu\text{g m}^{-3}$), we can calculate the mass absorption efficiency of EC (MAE) for each sample as

$$\text{MAE} = \frac{b_{\text{abs,Sunset}}}{\text{EC}} \quad (7)$$

3. Application of the method

3.1. Field campaign

In September and October 2014, a field campaign at the Cabauw Experimental Site for Atmospheric Research (CESAR)¹ (the Netherlands) was organised for the OC/EC-standardisation working group of CEN (European Committee for Standardisation). Following Ram and Sarin (2009), we have used the transmission measurement of the thermal optical analysis to calculate the attenuation coefficient using the data obtained from the field campaign. During the field campaign, two high volume samplers (Leckel SEQ47/50, 38 L/min) have sampled filters (Pallflex[®] Tissuquartz[™]) for OC/EC analysis with a sampling time of 24 h. Both high volume samplers had a cut off at $\text{PM}_{2.5}$. The air was not dried before sampling. The samples were stored in a cooler before analysis. Filters from both samplers and 20 different days were analysed. Six punches are taken from each filter sample, two of these are analysed using the EUSAAR2 protocol (Cavalli et al., 2010), two using the NIOSH890 protocol (Peterson and Richards, 2002) and two using the IMPROVE_A protocol (Chow et al., 2007). We thus have for every sampling day 12 samples available, which results in a total of 240 samples. The average EC masses are $2.13 \mu\text{g}/\text{cm}^2$ for EUSAAR, $1.86 \mu\text{g}/\text{cm}^2$ for NIOSH and $2.60 \mu\text{g}/\text{cm}^2$ for IMPROVE_A. The variation between the different protocols is then 17%. However, the protocol is irrelevant for obtaining the attenuation coefficient. During the campaign, the absorption coefficient was obtained using three co-located MAAPs ($\lambda = 670 \text{ nm}$). The MAAP sampling conditions were identical to that of the filter loading, i.e. with a $\text{PM}_{2.5}$ cut off determined and the air

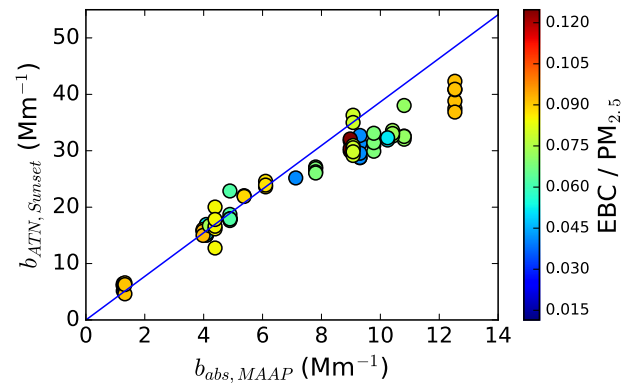


Fig. 1. The attenuation coefficient measured with the carbon analyser plotted versus the absorption coefficient measured with the MAAP. The plotted points are the samples with a cold start from the Cabauw campaign. The line that is added as a guide to the eye ($y = 3.87x$), represents a situation in which no overloading occurs. In colours, fractional contribution of EBC to $\text{PM}_{2.5}$ is indicated. (For interpretation of the references to colour in this figure legend, the reader is referred to the web version of this article.)

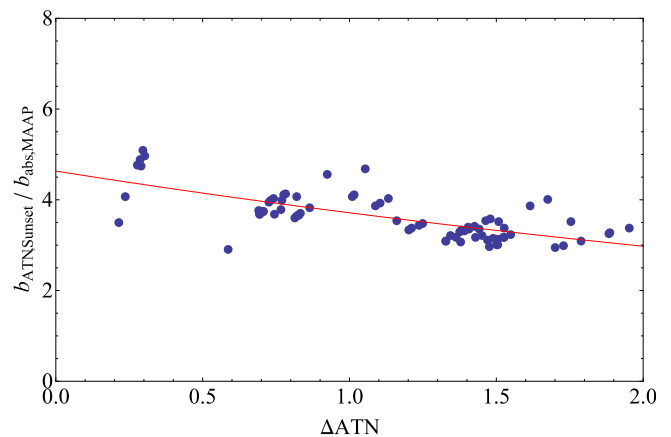


Fig. 2. The results of the calibration for 77 Cabauw samples. For each measurement, the ratio between $b_{\text{ATN,Sunset}}$ and $b_{\text{abs,MAAP}}$ is given by the blue dots. The red line is the best exponential fit for the function $C \cdot R(\Delta \text{ATN})$ and is given by $C \cdot R(\Delta \text{ATN}) = 4.63 \exp(-0.22 \Delta \text{ATN})$. (For interpretation of the references to colour in this figure legend, the reader is referred to the web version of this article.)

was not dried before sampling. The coefficient of variation between the three MAAPs was 3.8%, which is comparable to the unit-to-unit variability of 3% found by Müller et al. (2011).

Andersson et al. (2011) found some sensitivities in the transmission signal at the end of the measurement in the carbon analyser. Therefore, they did not use the transmission at the end of the measurement to determine I_{T_w} . Because we found some sensitivities as well in some carbon analysers that were involved in the CEN campaign (Ammerlaan et al., 2015), we have used blank filter measurements to determine I_{T_w} . Every day that analyses were performed also blank filters from the same batch were analysed. The analysis of the filters from the field campaign was done over a period of 32 days. For all the blanks that started with a cold oven and thus a stable transmission signal, we averaged the transmission signal over the first 60 s. An average over all these blanks, 20 in total, was finally taken to obtain I_{T_w} . The coefficient of variation was 5.6%, a more detailed review of the precision is given in Sect. 3.4 and the Supplementary Information.

During the dark start of a measurement, the transmission signal in our analyser was sensitive to the temperature. The transmission

¹ <http://www.cesar-observatory.nl/>.

through a filter was lower at a higher temperature. By extending the cooling period after the preceding measurement, the transmission stabilised. To be certain, we have therefore only selected samples with a ‘cold start’ (with a temperature below 35 °C). After the selection, 77 samples remained.

If an analyser does not show temperature sensitivities, Ammerlaan et al. (2015) provide suggestions how to test for such sensitivities, it is recommended to use the transmission at the end of a measurement as I_{T_w} . The advantage of taking the same filter and analysis for I_{T_w} and I_{T_d} is that the measurement of the attenuation coefficient becomes more precise (see Supplementary Information).

We have calculated the attenuation coefficients for the 77 Cabauw samples with the carbon analyser ($\lambda = 656$ nm) and plotted these coefficients as a function of the averaged absorption coefficient determined by the three MAAPs in Fig. 1. To illustrate the filter loading the ratio of EBC ($= b_{\text{abs,MAAP}}/6.6$) to $\text{PM}_{2.5}$ is plotted as a colour scale.

In Fig. 1, b_{ATN} ranges from 4.3 to 43 Mm^{-1} , the corresponding measured attenuation difference ranges from about 0.2 to 2. According to Müller et al. (2011), some of our samples are in the regime where loading may become important for some filters or instruments. Indeed a small loading effect is present and visualised by the levelling off. This loading effect will be accounted for in the calibration by evaluating the ratio of $b_{\text{ATN,Sunset}}$ to $b_{\text{abs,MAAP}}$, see Sect. 3.2. The filter tape in the MAAP is changed timely so that a loading effect is absent in MAAP data.

The levelling off seems to be associated with the amount of absorbing aerosol on the filter. We do not observe an apparent association to the $\text{PM}_{2.5}$ load or fractional contribution of EBC to $\text{PM}_{2.5}$ (colours in Fig. 1).

3.2. Calibration

For every sample, we have calculated the ratio between $b_{\text{ATN,Sunset}}$ and $b_{\text{abs,MAAP}}$ and plotted the ratio for all 77 selected samples in Fig. 2.

To parametrise $C \cdot R(\Delta\text{ATN})$, we have chosen for the simple function, $C \cdot R(\Delta\text{ATN}) = C \exp(-b \Delta\text{ATN})$, and used the routine *NonlinearModelFit* in Wolfram *Mathematica 9.0*[®] (see Fig. 2).

The fit yields the correction function for Cabauw, which is $C \cdot R(\Delta\text{ATN}) = 4.63 \exp(-0.22 \Delta\text{ATN})$. The parameters of the calibration are $C = 4.63 \pm 0.13$ and $R(\Delta\text{ATN}) = \exp(-0.22 \pm 0.02) \Delta\text{ATN}$

3.3. Absorption coefficient and mass absorption efficiency

We have calculated the absorption coefficient determined with our carbon analyser for an independent data set, which was also collected at the CESAR observatory near Cabauw, the Netherlands, and covers the period 29 June to 13 July, 2010. We have chosen these data, because simultaneous and co-located OC/EC data and MAAP data were available. For OC/EC analysis with the thermal optical carbon analyser, 17 samples collected at 15 different days are available. The MAAP is continuously operational. For each sample, the attenuation coefficient is determined with the Sunset Thermal Optical Carbon Analyser following the EUSAAR2 protocol (Cavalli et al., 2010). To obtain the absorption coefficient, the correction function for Cabauw (Sect. 3.2) $C \cdot R(\Delta\text{ATN}) = 4.63 \exp(-0.22 \Delta\text{ATN})$ is applied. The so obtained absorption coefficients are directly compared the MAAP absorption coefficients in Fig. 3.

We note that the absorption coefficient measured with the

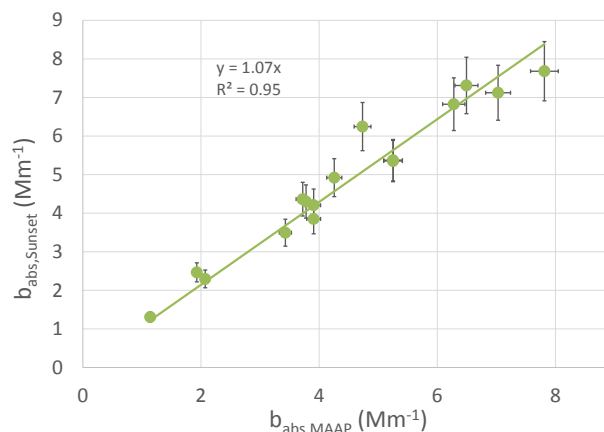


Fig. 3. The absorption coefficients of an independent data set from 2010 determined with a carbon analyser. The absorption coefficients determined with the carbon analyser are compared to the MAAP absorption coefficients, sampled at the same place and time. The error bars are the uncertainties calculated according to Sect. 3.4.

carbon analyser is biased high by 7% with respect to the MAAP. We consider this bias acceptable as differences between absorption photometers of different type are generally larger than 7% (Müller et al., 2011; Sheridan et al., 2005). These results are promising and indicate that the calibration may be stable over long periods.

We are now equipped with a method to obtain the absorption coefficient and EC mass concentrations from a single instrument. The ratio of these parameters is the MAE (Eq. (7)). For all 17 samples, the mass absorption efficiency MAE is plotted in Fig. 4a. We note that the MAE is not constant and varies in time. This variability is larger than the magnitude of the error bars (see Sect. 3.4), hence the temporal variation is likely real and allows to determine variations in this important aerosol property. For 2014 the MAE values are also calculated and plotted in Fig. 4b.

There is a remarkable difference between the MAE values of summer 2010 and autumn 2014. Apparently the atmospheric EC is absorbing light more efficiently in 2014. The independent MAAP observations confirm the higher absorption coefficients in 2014 as compared to 2010 (Table 1). On the other hand, total carbon (TC) and EC are lower in 2014. The EC concentrations of 2014 are confirmed by the partners in the CEN activity and also for 2010 no errors are found. The relatively higher contribution of OC to TC may explain only part of the higher absorption efficiency in 2014. The first two weeks of July 2010 continental winds advected exceptionally warm and dry air to the Netherlands. Therefore, we speculate that potentially condensable species that may enhance light absorption such as aerosol nitrate equilibrated towards the gas phase. Absorption enhancement by organic and inorganic coatings is thus minimal in 2010. In autumn 2014, temperatures were much lower especially at night time so that formation of coatings is more likely. Hence, despite the remarkable difference between MAE values in the different periods, we assume that the observed differences are real.

Coatings of secondary (in)organics on black carbon cores enhances the MAE. A series of intensive ambient air experiments with identical sampling and analysis protocols gave MAE values ranging from 6 to 39 $\text{m}^2 \text{g}^{-1}$, where the highest values were found in a biomass burning campaign (Quinn and Bates, 2005). Recently, Zanatta et al. (2016) observed at European stations a mean MAE of 10.0 $\text{m}^2 \text{g}^{-1}$ with minimum and maximum annual geometric means of 6.5 $\text{m}^2 \text{g}^{-1}$ and 17.3 $\text{m}^2 \text{g}^{-1}$, respectively. Lack and Cappa (2010) determined a MAE enhancement of 1.4 by measuring MAE values of

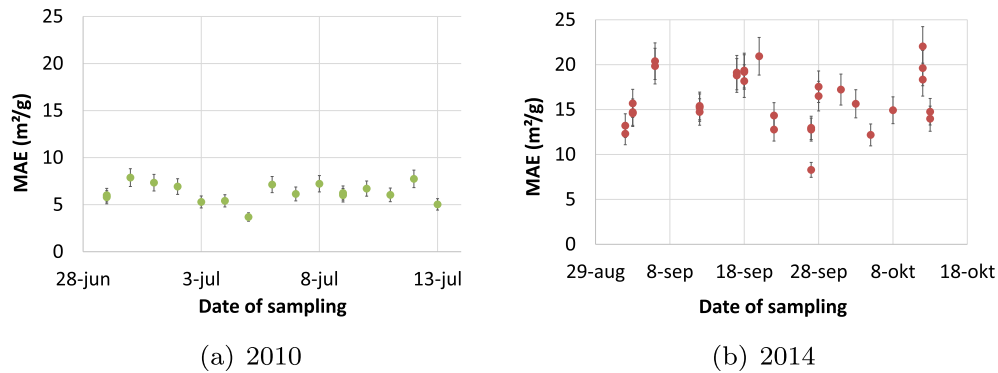


Fig. 4. The mass absorption efficiency for the Cabauw samples in 2010 and 2014. The mass absorption efficiency is calculated by using the carbon analyser and the calibration function $C \cdot R(ATN)$. The error bars are the uncertainties calculated according to Sect. 3.4.

Table 1
Comparison of 2010 and 2014 data.

Quantity	2010	2014
$b_{\text{abs,Sunset}}$ (Mm^{-1})	4.7 ± 1.9	6.8 ± 2.9
$b_{\text{abs,MAAP}}$ (Mm^{-1})	4.4 ± 1.0	7.1 ± 3.2
EC ($\mu\text{g m}^{-3}$)	0.73 ± 0.23	0.44 ± 0.21
EC/TC	0.19 ± 0.03	0.16 ± 0.04
MAE ($\text{m}^2 \text{g}^{-1}$)	6.3 ± 1.1	15.7 ± 2.8

originally internally mixed biomass burning particles and measuring MAE again after the coating was removed. Coatings of different refractive species or different coating thicknesses contribute to the observed variability in MAE values.

3.4. Precision

We have performed experiments to estimate the precision of the measurement of absorption properties of carbonaceous aerosol with a carbon analyser. The precisions are given in Table 2. In this section, we summarise the results of our estimates. A more detailed description of the experiments and calculations can be found in the [Supplementary Information](#).

We have estimated the precisions in the absorption coefficients and MAE for three methods. If I_{T_w} is calculated on the basis of instrument blank filters, the precision of the absorption coefficient and the MAE are 10% and 12%, respectively. The uncertainty is caused by uncertainties in the MAAP (3%), the determination of EC (7.2%) and the determination of the transmission of light (2%–5.5%). For a very stable laser signal, contributions from inter-filter variability are avoided. The precisions of the absorption coefficient and the MAE using this method are 4% and 8%, respectively. Finally, we have an ‘alternative’ estimate, based on the experimental data in Fig. 3. The precision in the absorption coefficient in the data is 9.4%. This alternative precision estimate supports the bottom-up precision estimates discussed here above.

4. Discussion

In this work we observe a loss in linearity between the absorption coefficient measured with the MAAP and the attenuation coefficient measured with the carbon analyser. This loss of linearity is caused by a reduced optical path length in the filter (loading effect or ‘shadowing effect’) and is accounted for in the calibration. The levelling off becomes apparent when the attenuation coefficient of the carbon analyser is above about 25 Mm^{-1} or about $4.5 \mu\text{gC cm}^{-2}$. In the Himalayas, [Ram et al. \(2010a\)](#) observed

Table 2

The precision of the MAE and $b_{\text{abs,Sunset}}$ calculated for three different methods. The calculation with ‘different filter’ represents the method where I_{T_w} is calculated on the basis of instrument blank filters. The calculation with ‘same filter’ represents the method of a very stable laser signal that allows determination of I_{T_b} and I_{T_w} from the same filter sample, thereby avoiding contributions from inter-filter variability. The ‘alternative’ calculation is based on the experimental data shown in Fig. 3.

Quantity	Different filter	Same filter	Alternative
$b_{\text{abs,Sunset}}$	10%	4%	9.4%
MAE	12%	8%	

overloading with respect to transmission when concentrations became higher than $1 \mu\text{gC m}^{-3}$, for 24 h of high volume sampling this also corresponds to a filter surface loading of about $2.8 \mu\text{gC cm}^{-2}$. At an urban location, [Ram et al. \(2010b\)](#) observed a linear relationship between the transmission and the filter surface loading, when EC surface loading were kept below $8.0 \mu\text{gC cm}^{-2}$. Thus, when the EC surface loading is kept below $2 \mu\text{gC cm}^{-2}$, calibration of the carbon analyser absorption photometer can be reduced to a single parameter C . However, in practice, EC measurements become more uncertain at such low surface loadings.

[Collaud Coen et al. \(2010\)](#) have found that the value of C for Cabauw varies with the season or was changed because a modification to the inlet. The value found in our calibration for Cabauw, $C = 4.63 \pm 0.13$, is in line with the value ($C \sim 4.8$) found for the May–July period by [Collaud Coen et al.](#) The application of our method to an independent data set from 2010 showed that the calibration may be valid over a period of several years. The variation of C in different seasons and at different sites is not well understood at the moment, and we have only studied the summer period and one site in detail. From the application on the independent data, we can conclude that C may exhibit a low variability in time, since the calibration was applicable to a dataset collected 4 years earlier at the same location. We did not investigate spatial variability yet. However, some explorative calculations for other Dutch sites (not shown) pointed toward high spatial variability as found by [Collaud Coen et al. \(2010\)](#). More research on the variation in C over longer periods and at different sites needs to be performed. The calibration added to the method of measuring light absorption with a carbon analyser should help in studying the variation in C .

The mass absorption efficiency of EC is the ratio of absorption coefficient to the mass concentration of EC. The MAE thus depends on the uncertainties and absolute values of both parameters. The MAAP is a reliable instrument that compares well to reference absorption measurements, i.e. to the average of a photo-acoustic measurement and extinction minus scattering measurement in the Reno Aerosol Optics Study ([Sheridan et al., 2005](#)). However,

when organic aerosol is abundantly present, filter based absorption measurements are overestimating light absorption as compared to more direct photo-acoustic measurements (Lack et al., 2008; Cappa et al., 2008). For EC mass concentrations, several widely applied thermal-optical analysis protocols exist that result in significant differences in the OC to EC differentiation (Cheng et al., 2011). At higher starting temperatures of the OC/EC analysis, coatings may be volatilised before the absorption measurement is done. The start of this analysis thus should be at cold oven to ensure a better determination of the absorption.

The precisions found on the basis of the scatter in the data are comparable to the estimated precisions estimated (Table 2), which supports our confidence in the estimated precisions in Sect. 3.4. The best precisions are obtained when I_{T_w} and I_{T_d} are determined from the same analysis run, which is possible when the transmission signal of the carbon analyser is stable enough. This results in a precision of the absorption coefficient of 3.7% and a precision in the MAE of 8.1%. However, if the laser transmission signal of the analyser is not stable enough, these precisions are not achievable. In that situation, the precisions are 9.9% and 12.3% for the absorption coefficient and the MAE, respectively. The precisions for a stable laser signal in the analyser can be improved further by placing the quartz boat into the oven as horizontal as possible. A technical adjustment could be supportive to this.

Our work shows that the mass absorption efficiency (MAE) of carbonate aerosol can be determined with a carbon analyser with a precision of 12.3%. The absorption coefficient can be determined with a precision of 9.9%, which is in the same order as unit-to-unit variability of Aethalometer absorption photometers (Müller et al., 2011). So far, we applied the method only to a limited set of data, nevertheless, our results show that extended application of this method is likely to yield valuable insights in the efficiency of aerosols to absorb shortwave radiation.

Acknowledgements

This work performed within the project ACTRIS-II that has received funding from the European Unions Horizon 2020 research and innovation programme under grant agreement No 654109.

The authors further would like to thank the European Committee for Standardisation (CEN) for the usage of data sampled for the standardisation work by CEN/TC264/WG35 on OC/EC analysis.

Appendix A. Supplementary data

Supplementary data related to this article can be found at <http://dx.doi.org/10.1016/j.atmosenv.2017.05.031>.

References

Ammerlaan, B.A.J., Jedynska, A.D., Henzing, J.S., Holzinger, R., 2015. On a possible bias in elemental carbon measurements with the Sunset thermal/optical carbon analyser caused by unstable laser signal. *Atmos. Environ.* 122, 571–576.

Andersson, A., Sheesley, R.J., Kirillova, E.N., Gustafsson, Ö., 2011. An algorithm for retrieving black carbon optical parameters from thermal-optical (OC/EC) instruments. *Atmos. Meas. Tech. Discuss.* 4 (1), 1233–1254.

Arnott, W.P., Hamasha, K., Moosmüller, H., Sheridan, P.J., Ogren, J.A., 2005. Towards aerosol light-absorption measurements with a 7-wavelength aethalometer: evaluation with a photoacoustic instrument and 3-wavelength nephelometer. *Aerosol Sci. Technol.* 39 (1), 17–29.

Ballach, J., Hitznerberger, R., Schultz, E., Jaeschke, W., 2001. Development of an improved optical transmission technique for black carbon (bc) analysis. *Atmos. Environ.* 35 (12), 2089–2100.

Bond, T.C., Anderson, T.L., Campbell, D., 1999. Calibration and intercomparison of filter-based measurements of visible light absorption by aerosols. *Aerosol Sci. Technol.* 30 (6), 582–600.

Bond, T.C., Doherty, S.J., Fahey, D.W., Forster, P.M., Bernsten, T., DeAngelo, B.J., Flanner, M.G., Ghan, S., Krcher, B., Koch, D., Kinne, S., Kondo, Y., Quinn, P.K., Sarofim, M.C., Schultz, M.G., Schulz, M., Venkataraman, C., Zhang, H., Zhang, S.,

Bellouin, N., Guttikunda, S.K., Hopke, P.K., Jacobson, M.Z., Kaiser, J.W., Klimont, Z., Lohmann, U., Schwarz, J.P., Shindell, D., Storelvmo, T., Warren, S.G., Zender, C.S., 2013. Bounding the role of black carbon in the climate system: a scientific assessment. *J. Geophys. Res. Atmos.* 118 (11), 5380–5552.

Cappa, C.D., Lack, D.A., Burkholder, J.B., Ravishankara, A., 2008. Bias in filter-based aerosol light absorption measurements due to organic aerosol loading: evidence from laboratory measurements. *Aerosol Sci. Technol.* 42 (12), 1022–1032.

Cavalli, F., Viana, M., Yttri, K.E., Genberg, J., Putaud, J.P., 2010. Toward a standardised thermal-optical protocol for measuring atmospheric organic and elemental carbon: the esaar protocol. *Atmos. Meas. Tech.* 3 (1), 79–89.

Cheng, Y., He, K.B., Zheng, M., Duan, F.K., Du, Z.Y., Ma, Y.L., Tan, J.H., Yang, F.M., Liu, J.M., Zhang, X.L., et al., 2011. Mass absorption efficiency of elemental carbon and water-soluble organic carbon in Beijing, China. *Atmos. Chem. Phys.* 11 (22), 11497–11510.

Chow, J.C., Watson, J.G., Chen, L.W.A., Chang, M.C.O., Robinson, N.F., Trimble, D., Kohl, S., 2007. The improve_a temperature protocol for thermal/optical carbon analysis: maintaining consistency with a long-term database. *J. Air & Waste Manag. Assoc.* 57 (9), 1014–1023.

Collaud Coen, M., Weingartner, E., Apituley, A., Ceburnis, D., Fierz-Schmidhauser, R., Flentje, H., Henzing, J.S., Jennings, S.G., Moerman, M., Petzold, A., Schmid, O., Baltensperger, U., 2010. Minimizing light absorption measurement artifacts of the aethalometer: evaluation of five correction algorithms. *Atmos. Meas. Tech.* 3 (2), 457–474.

Hansen, A.D.A., Rosen, H., Novakov, T., 1984. The aethalometer instrument for the real-time measurement of optical absorption by aerosol particles. *Sci. Total Environ.* 36, 191–196.

Lack, D.A., Cappa, C.D., 2010. Impact of brown and clear carbon on light absorption enhancement, single scatter albedo and absorption wavelength dependence of black carbon. *Atmos. Chem. Phys.* 10 (9), 4207–4220.

Lack, D.A., Cappa, C.D., Covert, D.S., Baynard, T., Massoli, P., Sierau, B., Bates, T.S., Quinn, P.K., Lovejoy, E.R., Ravishankara, A., 2008. Bias in filter-based aerosol light absorption measurements due to organic aerosol loading: evidence from ambient measurements. *Aerosol Sci. Technol.* 42 (12), 1033–1041.

Liousse, C., Cachier, H., Jennings, S.G., 1993. Optical and thermal measurements of black carbon aerosol content in different environments: variation of the specific attenuation cross-section, sigma (σ). *Atmos. Environ. Part A General Top.* 27 (8), 1203–1211.

Moosmüller, H., Chakrabarty, R.K., Arnott, W.P., 2009. Aerosol light absorption and its measurement: a review. *J. Quantitative Spectrosc. Radiat. Transf.* 110 (11), 844–878.

Müller, T., Henzing, J.S., de Leeuw, G., Wiedensohler, A., Alastuey, A., Angelov, H., Bizjak, M., Collaud Coen, M., Engström, J.E., Gruening, C., Hillamo, R., Hoffer, A., Imre, K., Ivanow, P., Jennings, G., Sun, J.Y., Kalivitis, N., Karlsson, H., Komppula, M., Laj, P., Li, S.M., Lunder, C., Marinoni, A., Martins dos Santos, S., Moerman, M., Nowak, A., Ogren, J.A., Petzold, A., Pichon, J.M., Rodriguez, S., Sharma, S., Sheridan, P.J., Teinilä, K., Tuch, T., Viana, M., Virkkula, A., Weingartner, E., Wilhelm, R., Wang, Y.Q., 2011. Characterization and intercomparison of aerosol absorption photometers: result of two intercomparison workshops. *Atmos. Meas. Tech.* 4 (2), 245–268.

Müller, T., Virkkula, A., Ogren, J.A., 2014. Constrained two-stream algorithm for calculating aerosol light absorption coefficient from the particle soot absorption photometer. *Atmos. Meas. Tech.* 7 (12), 4049–4070.

Peterson, M.R., Richards, M.H., 2002. Thermal-optical-transmittance analysis for organic, elemental, carbonate, total carbon, and OCX2 in PM_{2.5} by the EPA/NIOSH method. In: *Proceedings, Symposium on Air Quality Measurement Methods and Technology-2002*. Air & Waste Management Association, Pittsburgh, PA, pp. 83–91.

Petzold, A., Ogren, J.A., Fiebig, M., Laj, P., Li, S.M., Baltensperger, U., Holzer-Popp, T., Kinne, S., Pappalardo, G., Sugimoto, N., Wehrli, C., Wiedensohler, A., Zhang, X.Y., 2013. Recommendations for reporting “black carbon” measurements. *Atmos. Chem. Phys.* 13 (16), 8365–8379.

Petzold, A., Schönlinner, M., 2004. Multi-angle absorption photometry a new method for the measurement of aerosol light absorption and atmospheric black carbon. *J. Aerosol Sci.* 35 (4), 421–441.

Quinn, P., Bates, T., 2005. Regional aerosol properties: comparisons of boundary layer measurements from ace 1, ace 2, aerosols99, indoex, ace asia, tarfox, and neaqs. *J. Geophys. Res. Atmos.* 110 (D14).

Ram, K., Sarin, M., Hegde, P., 2010a. Long-term record of aerosol optical properties and chemical composition from a high-altitude site (manora peak) in central himalaya. *Atmos. Chem. Phys.* 10 (23), 11791–11803.

Ram, K., Sarin, M., Tripathi, S., 2010b. Inter-comparison of thermal and optical methods for determination of atmospheric black carbon and attenuation coefficient from an urban location in northern India. *Atmos. Res.* 97 (3), 335–342.

Ram, K., Sarin, M.M., 2009. Absorption coefficient and site-specific mass absorption efficiency of elemental carbon in aerosols over urban, rural, and high-altitude sites in India. *Environ. Sci. Technol.* 43 (21), 8233–8239.

Reid, J.S., Hobbs, P.V., Liousse, C., Martins, J.V., Weiss, R.E., Eck, T.F., 1998. Comparisons of techniques for measuring shortwave absorption and black carbon content of aerosols from biomass burning in Brazil. *J. Geophys. Res. Atmos.* (1984–2012) 103 (D24), 32031–32040.

Sheridan, P.J., Arnott, W.P., Ogren, J.A., Andrews, E., Atkinson, D.B., Covert, D.S., Moosmüller, H., Petzold, A., Schmid, B., Strawa, A.W., Varma, R., Virkkula, A., 2005. The Reno Aerosol Optics Study: an evaluation of aerosol absorption measurement methods. *Aerosol Sci. Technol.* 39 (1), 1–16.

Turpin, B.J., Cary, R., Huntzicker, J., 1990. An in situ, time-resolved analyzer for

- aerosol organic and elemental carbon. *Aerosol Sci. Technol.* 12 (1), 161–171.
- Virkkula, A., Ahlquist, N.C., Covert, D.S., Arnott, W.P., Sheridan, P.J., Quinn, P.K., Coffman, D.J., 2005. Modification, calibration and a field test of an instrument for measuring light absorption by particles. *Aerosol Sci. Technol.* 39 (1), 68–83.
- Weingartner, E., Saathoff, H., Schnaiter, M., Streit, N., Bitnar, B., Baltensperger, U., 2003. Absorption of light by soot particles: determination of the absorption coefficient by means of aethalometers. *J. Aerosol Sci.* 34 (10), 1445–1463.
- Zanatta, M., Gysel, M., Bukowiecki, N., Müller, T., Weingartner, E., Areskoug, H., Fiebig, M., Yttri, K., Mihalopoulos, N., Kouvarakis, G., Beddows, D., Harrison, R., Cavalli, F., 2016. A european aerosol phenomenology-5: climatology of black carbon optical properties at 9 regional background sites across europe. *Atmos. Environ.* 145, 346–364.